5372–5378 *Nucleic Acids Research, 1998, Vol. 26, No. 23*

The role of the T-box for the function of the vitamin D receptor on different types of response elements

Marcus Quack, Karol Szafranski, Juha Rouvinen[1] and Carsten Carlberg*

Institut für Physiologische Chemie I and Biomedizinisches Forschungszentrum, Heinrich-Heine-Universität, D-40001 Düsseldorf, Germany and [1]Department of Chemistry, University of Joensuu, FIN-80101 Joensuu, Finland

Received August 10, 1998; Revised and Accepted October 13, 1998

ABSTRACT

The nuclear hormone 1α,25-dihydroxyvitamin D_3 (VD) mainly functions through a heterodimer formed between the VD receptor (VDR) and the retinoid X receptor (RXR). This transcription factor complex specifically recognizes DNA sequences, referred to as VD response elements (VDREs), that are formed by two hexameric core binding motifs arranged either as direct repeats spaced by 3 nt (DR3) or inverted palindromes with nine intervening nucleotides (IP9). Gel shift clipping assays provided the first evidence that VDR–RXR heterodimers form different conformations on these two types of VDREs. Since the T-box within the C-terminal extension of the receptor DNA binding domain (DBD) was previously shown to form a dimerization interface with the partner receptor DBD when bound to DR-type response elements, all six amino acid residues of the VDR T-box were investigated for their role in VDR–RXR heterodimer complex formation on DR3- and IP9-type VDREs. Interestingly, the residue Phe93 (F93) was found to be critical on both types of VDREs, whereas the role of the residue Ile94 (I94) was found to depend on ionic strength of the binding reaction and the nature of the VDRE. However, under physiological conditions I94 was also shown to be critical on both VDRE types. The monitored differences between the two VDR-containing protein–DNA complexes helps in an understanding of the differential action of the nuclear hormone VD and its therapeutically important analogues.

INTRODUCTION

The lipophilic hormone 1α,25-dihydroxyvitamin D_3 (VD), the biologically active form of vitamin D_3, acts through binding and activation of the nuclear VD receptor (VDR) (1). VDR is a member of a superfamily of structurally related nuclear receptor transcription factors (2) that binds to specific sequences in the promoter of VD target genes, commonly referred to as VD response elements (VDREs) (3). VD is involved in the regulation of a variety of important biological functions, such as calcium homeostasis (4), as well as cellular growth, differentiation and apoptosis (5). These properties provide VD with an interesting therapeutic potential against a variety of diseases, such as osteoporosis, cancer and psoriasis (6), however, a more selective biological profile of the hormone, e.g. a potent antiproliferative effect without a calcemic side-effect in parallel, would be desired. This goal could be achieved by dissecting nuclear VD signalling into different pathways that may be selectively activated by analogues of VD. The model of multiple VD signalling pathways (7) suggests that the pleiotropic function of VD is based on a variety of dimeric VDR complexes bound to different types of VDREs. According to the model, each of these VDR-containing protein–DNA complexes may represent one function of VD, i.e. that such kinds of complexes may preferentially be found in the regulatory region of those genes that mediate the respective function of the hormone. In support of this model the first VDRE-selective VD analogues have been identified (8).

Simple VDREs are formed by two hexameric core binding sites of the consensus sequence RGKTSA (R = A or G; K = G or T; S = C or G), as the VDR binds to DNA as a homo- or heterodimeric complex. The main partner receptor for the VDR is the retinoid X receptor (RXR), which is the nuclear receptor for 9-*cis*-retinoic acid (9,10). VDR–RXR heterodimers bind preferentially to DR3-type VDREs or to IP9-type VDREs (11). On DR3-type VDREs they bind in a non-symmetrical head-to-tail tandem arrangement, where VDR binds in most cases to the 3′-motif (12,13). In contrast, like all palindromic sequences, IP9-type VDREs are *per se* symmetrical, since the heterodimeric partner receptors bind in a tail-to-tail arrangement. However, natural IP-type response elements were found to be sufficiently asymmetrical in their core binding sequences to allow polarity-determined binding of heterodimers (12,14).

Nuclear receptors contain a ligand-binding domain (LBD) in their C-terminal half, that also mediates transactivation and DNA-independent dimerization, and a DNA-binding domain (DBD), that is formed by two zinc finger structures in their N-terminal part. The DBD and the LBD are linked by a hinge region of 35–50 residues that form a long α-helical structure according to the crystal structure of the thyroid hormone receptor (T_3R) DBD (15). The loop between this α-helix and the second zinc finger contains a short six residue region, referred to as the T-box (16,17), which has been suggested to form a dimerization interface for the interaction with the RXR DBD (15,18,19). A specific and directed dimerization of the DBDs appears to be the major discriminative parameter for a selective recognition of response elements with properly spaced core binding domains. The high conservation of the DBDs of T_3R and VDR allows an assumption to be made that the same principles also hold true for VDR–RXR heterodimers.

*To whom correspondence should be addressed at: Institut für Physiologische Chemie I, Heinrich-Heine-Universität Düsseldorf, Postfach 10 10 07, D-40001 Düsseldorf, Germany. Tel: +49 211 8115358; Fax: +49 211 208399; Email: carlberg@uni-duesseldorf.de

VDR–RXR heterodimers bound to DR3- and IP9-type VDREs appear to be the most important VDR-containing complexes that have to be discriminated in the model of multiple VD signalling pathways (1,7,11). Therefore, in this report characteristic differences between these two complex types were investigated. Band shift clipping assays provided the first experimental proof that VDR takes a different conformation in each of these complexes. Functional analysis of a series of VDR T-box mutants has highlighted residues F93 and I94 as critical components in the DNA-directed interaction between VDR and RXR.

MATERIALS AND METHODS

DNA constructs

The cDNA for human VDR and human RXRα were subcloned into the pSG5 expression vector (Stratagene) (20). The VDR construct was used as template for a linear PCR reaction using native *Pfu* DNA polymerase (Stratagene) with a profile of 1 min at 94°C, 1 min at 55°C and 11 min at 68°C for 16 cycles. The following primer pairs were used for the M90A, K91A, E92A, F93A, I94A and L95A point mutations (M, methionine; K, lysine; E, glutamic acid; L, leucine): M90A+ (GTGGACATCGGCATGG-CGAAGGAGTTCATTCTG) and M90A– (CAGAATGAACTC-CTTCGCCATGCCGATGTCCAC); K91A+ (ATCGGCATGAT-GGCGGAGTTCATTCTG) and K91A– (CAGAATGAACTCC-GCCATCATGCCGAT); E92A+ (GGCATGATGAAGGCGTT-CATTCTGACA) and E92A– (TGTCAGAATGAACGCCTTC-ATCATGCC); F93A+ (ATGATGAAGGAGGCCATTCTGAC-AGATGAG) and F93A– (CTCATCTGTCAGAATGCCCTCC-TTCATCAT); I94A+ (ATGAAGGAGTTCGCTCTGACAGAT-GAG) and I94A– (CTCATCTGTCAGAGCGAACTCCTTCAT); L95A+ (ATGAAGGAGTTCATTGCGACAGATGAGGAAGTG) and L95– (CACTTCCTCATCTGTCGCAATGAACTCCTTCAT).

Methylated parental DNA was then digested selectively with *Dpn*I and supercompetent *Escherichia coli* XL-1 (Stratagene) were transformed with non-digested, PCR-generated plasmid DNA. The respective point mutations were confirmed by sequencing. The fusion of the DR3-type VDRE from the rat atrial natriuretic factor (ANF) gene promoter and the IP9-type VDRE from the mouse c-*fos* promoter, respectively (sequences in Fig. 2A), were transferred together with the thymidine kinase (*tk*) promoter from the respective chloramphenicol acetyltransferase reporter gene constructs (21,22) into the promoterless luciferase reporter gene plasmid pGL2 (Promega).

Limited protease digestion assay

Linearized DNA from the pSG5-based constructs of VDR and RXRα were transcribed with T7 RNA polymerase and translated *in vitro* using rabbit reticulocyte lysate as recommended by the supplier (Promega). Equal amounts of *in vitro* translated [^{35}S]methionine-labelled VDR protein and unprogrammed lysate, [^{35}S]methionine-labelled RXR protein and unprogrammed lysate, ^{35}S-labelled VDR and non-labelled RXR proteins or non-labelled VDR and ^{35}S-labelled RXR proteins were mixed and incubated with 10 µM VD (or ethanol as control) for 15 min at room temperature in a total volume of 20 µl binding buffer [10 mM HEPES, pH 7.9, 1 mM DTT, 0.2 µg/µl poly(dI–dC) and 5% glycerol]. Approximately 1 ng of non-labelled DR3-type or IP9-type VDRE was added to the receptor/ligand mixture and incubation was continued for 20 min. Then the mixtures were incubated with the endoprotease chymotrypsin (final concentration 33 ng/µl; Boehringer Mannheim) for 15 min at room temperature. The digestion reactions were stopped by adding 20 µl protein gel loading buffer (0.25 M Tris, pH 6.8, 20% glycerol, 5% mercaptoethanol, 2% SDS, 0.025% w/v bromophenol blue). The samples were denatured at 95°C for 5 min and electrophoresed through a 15% SDS–polyacrylamide gel. The gels were dried and exposed to a BioMax film (Kodak) overnight.

Gel shift and gel shift clipping assays

Equal amounts of *in vitro* translated VDR (or VDR mutant) and RXR proteins or bacterially expressed GST–VDR fusion protein (VDR_{GST}; kindly provided by P.Polly) and *in vitro* translated RXR protein were mixed and incubated in the presence of the indicated concentrations of VD (or ethanol as control) for 15 min at room temperature in a total volume of 20 µl binding buffer. The buffer was adjusted to the indicated salt concentrations by addition of respective amounts of 1 M KCl. The DR3-type and the IP9-type VDREs were labelled by a fill-in reaction using [α-^{32}P]dCTP and the Klenow fragment of DNA polymerase I (Promega). Approximately 1 ng of labelled probe (50 000 c.p.m.) was added to the receptor/ligand mixture and incubation was continued for 20 min. In regular gel shift assays, protein–DNA complexes were resolved on a 5 or 8% non-denaturing polyacrylamide gel (at room temperature) in 0.5× TBE (45 mM Tris, 45 mM boric acid, 1 mM EDTA, pH 8.3). In gel shift clipping assays, the chymotrypsin was added to a final concentration of 33 ng/µl (or 132 ng/µl in the case of VDR_{GST}) and the incubation was continued for 15 min at room temperature. Then the partially digested protein–DNA complexes were resolved on an 8% non-denaturing polyacrylamide gel in 0.5× TBE. In both cases, the gels were dried and exposed to a Fuji MP2040S imager screen overnight. The ratio of free probe to protein–probe complexes was quantified on a Fuji FLA2000 reader using Image Gauge software (Raytest). Each condition was analysed, at least, in triplicate.

Transfection and luciferase assays

Cos-7 SV40-transformed African green monkey kidney cells were seeded into 6-well plates (10^5 cells/ml) and grown overnight in phenol red-free DMEM supplemented with 10% charcoal-treated fetal calf serum (FCS). Liposomes were formed by incubating 1 µg of the reporter plasmid, 0.25 µg each of pSG5-based receptor expression vectors for VDR (or VDR mutant) and RXR and 1 µg of the reference plasmid pCH110 (Pharmacia) with 15 µg *N*-[1-(2,3-dioleoyloxy)propyl]-*N*,*N*,*N*-trimethylammonium methylsulfate (DOTAP; Boehringer Mannheim) for 15 min at room temperature in a total volume of 100 µl. After dilution with 0.9 ml phenol red-free DMEM, the liposomes were added to the cells. Phenol red-free DMEM supplemented with 30% charcoal-treated FCS (500 µl) was added 4 h after transfection. At this time, VD (100 nM) or ethanol (0.1%) was also added. The cells were lysed 16 h after stimulation onset using the reporter gene lysis buffer (Boehringer Mannheim) and the constant light signal luciferase reporter gene assay was performed as recommended by the supplier (Boehringer Mannheim). The luciferase activities were normalized in proportion to β-galactosidase activity and induction factors were calculated as the ratio of luciferase activity of ligand-stimulated cells to that of solvent controls. The inducibility of VDR mutants were expressed in relation to that of VDR.

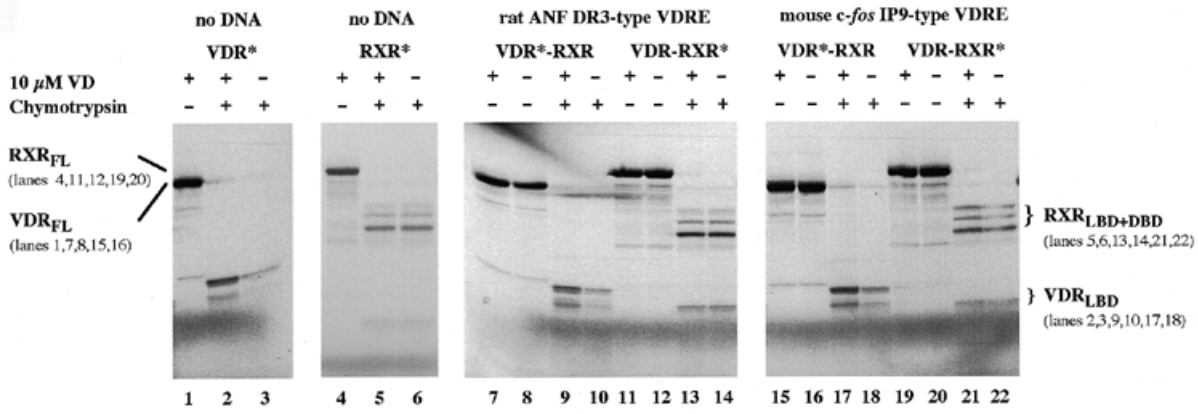

Figure 1. Limited protease digestion of VDR–RXR heterodimers on different VDRE types. Equal amounts of *in vitro* translated ^{35}S-labelled VDR protein (VDR*), ^{35}S-labelled RXR protein (RXR*), heterodimers between VDR* and non-labelled RXR proteins or heterodimers between non-labelled VDR and RXR* proteins were formed in the presence of 10 μM VD (or ethanol as control) on the non-labelled DR3-type VDRE from the rat ANF gene promoter or the IP9-type VDRE from the mouse c-*fos* gene promoter. After incubation with 33 ng/μl chymotrypsin the digestion products were resolved on a denaturing 15% SDS–polyacrylamide gel. The gels were dried and exposed to a BioMax film (Kodak) overnight. Non-digested VDR full-length protein (VDR_{FL}) is shown in lanes 1, 7, 8, 15 and 16, non-digested RXR full-length protein (RXR_{FL}) in lanes 4, 11, 12, 19 and 20, two digested VDR fragments (VDR_{LBD}) in lanes 2, 3, 9, 10, 17 and 18 and three digested RXR fragments ($RXR_{LBD+DBD}$) in lanes 5, 6, 13, 14, 21 and 22. A representative gel is shown.

RESULTS

Nuclear receptor conformations are often monitored by the limited protease digestion assay (23,24), a method that has also been established for the VDR (8,25). In the absence of DNA, the digestion of *in vitro* translated VDR with the endoprotease chymotrypsin provided two fragments (Fig. 1, lane 2) that represent major parts of the LBD (26) and indicate protease-resistant, ligand-stabilized receptor conformations (27). This pattern was not found to be significantly changed in the presence of *in vitro* translated RXR, the DR3-type VDRE of the rat ANF gene promoter (22) (lanes 9 and 10) or the IP9-type VDRE of the mouse c-*fos* gene promoter (21) (lanes 17 and 18). A similar effect was observed for the RXR digestion pattern, where no significant differences between the pattern obtained with RXR alone (lanes 5 and 6) and that of RXR in a complex with VDR and with either the DR3-type (lanes 13 and 14) or the IP9-type VDRE (lanes 21 and 22). This suggests that the limited protease digestion assay is not able to facilitate detection of a significant difference between isolated receptors and their heterodimeric complexes on DNA or to differentiate between the two VDRE types. Therefore, gel shift experiments were performed using VDR and RXR with both VDREs (Fig. 2B). The formation of VDR–RXR heterodimer–response element complexes in the binding reaction was improved in the presence of 10 μM VD in the binding reaction in comparison with ethanol-treated controls. When DNA-complexed VDR–RXR heterodimers were incubated with chymotrypsin prior to gel separation, a protein–DNA complex with a faster electrophoretic mobility, i.e. a smaller molecular mass, was observed. The difference between this gel shift clipping assay and the limited protease digestion assay (as described in Fig. 1) is that in the latter the protein and not the DNA is radiolabelled and that the reaction products of the gel shift clipping assay are resolved through a non-denaturing gel, where all other reaction conditions were kept constant. The complex observed in the gel shift clipping assay appeared to be identical in migration rate on both types of VDREs. However, in the presence of ligand, ~6% of the protein–DNA complex input displayed resistance against protease digestion on the IP9-type VDRE, whereas ~36% of the complexes remained stable on the DR3-type VDRE. This complex stabilization was clearly ligand-dependent, as 4- and 10-fold lower amounts of VDR–RXR–DNA complexes were found to be resistant to protease digestion in the absence of ligand. The difference in protection between the complexes on DR3-type and IP9-type VDREs against chymotrypsin digestion did not seem to depend on incubation time, but required protease amounts >16 ng/μl (data not shown). A similar experiment was then performed with heterodimers composed of bacterially expressed VDR_{GST} and *in vitro* translated RXR (Fig. 2C), which essentially provided the same results as with *in vitro* translated VDR, i.e. VDR–RXR heterodimers are less resistant to protease digestion when formed on a IP9-type VDRE than on a DR3-type VDRE. However, for digestion of the heterodimeric complexes higher chymotrypsin concentrations were required. Taken together, both experiment series indicated that VDR–RXR heterodimers could form different conformations on DR3- and IP9-type VDREs, each showing a characteristic sensitivity to the protease chymotrypsin that is modulated differently by ligand. Moreover, the lack of difference in the protease digestion patterns that were observed under the denaturing conditions of the limited protease digestion assay (Fig. 1) and the VDRE-dependent stability of protease-digested VDR–RXR heterodimers that were found under non-denaturing conditions of the gel shift clipping assay (Fig. 2) suggest that the interaction of the extended DBDs of VDR and RXR on DR3-type VDREs is clearly stronger than that on IP9-type VDREs.

In order to analyse the role of the six T-box residues M90, K91, E92, F93, I94 and L95 of the extended DBD of the VDR (Fig. 3A) in heterodimerization, each residue was individually mutated to an alanine. These six mutations were tested in gel shift experiments for heterodimerization with RXR in comparison with VDR_{wt} on the DR3- and the IP9-type VDRE, respectively (Fig. 3B). Quantification of the VDR–RXR–response element complexes (Fig. 3C) illustrated that on the DR3-type VDRE the F93 residue mutation only showed a significant effect on complex formation, whereas on the IP9-type VDRE the I94 residue mutation additionally resulted in a decrease in heterodimer binding. However, when testing these six T-box mutants in a reporter gene assay (Fig. 3D) both residues F93 and I94 appeared to play a significant role in the function of VDR–RXR heterodimers on both VDRE types.

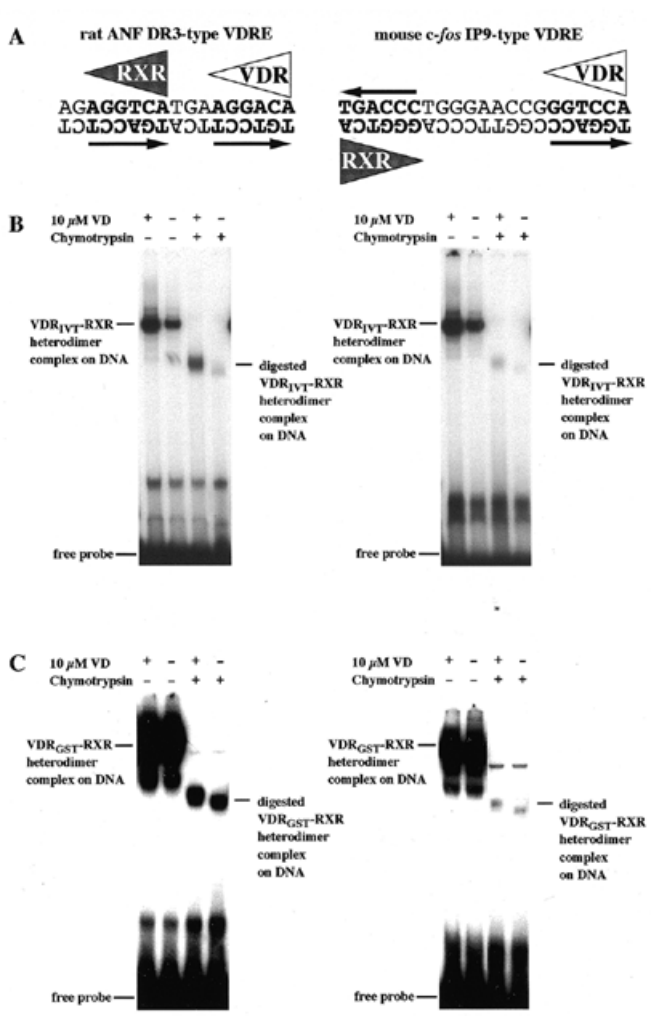

Figure 2. Different protease sensitivity of VDR–RXR heterodimers bound to DR3- and to IP9-type VDREs. Complex formation of the DBDs for VDR and RXR on both VDRE types is schematically depicted (the core binding motifs are in bold); the DBDs are represented by triangles in order to visualize their ordered orientation (**A**). Heterodimers of *in vitro* translated VDR (VDR_{IVT}) and RXR proteins (**B**) or heterodimers of bacterially expressed VDR_{GST} and *in vitro* translated RXR protein (**C**) were formed in the presence of 10 μM VD (or ethanol as control) on the ^{32}P-labelled rat ANF DR3-type VDRE or the mouse c-*fos* IP9-type VDRE. The experiments were performed at a salt concentration of 100 mM. One half of the samples were then incubated with 33 ng/μl chymotrypsin (or 132 ng/μl in the case of VDR_{GST}) for 15 min at room temperature. Protein–DNA complexes were separated from free probe on an 8% non-denaturing polyacrylamide gel. Representative experiments are shown (B and C).

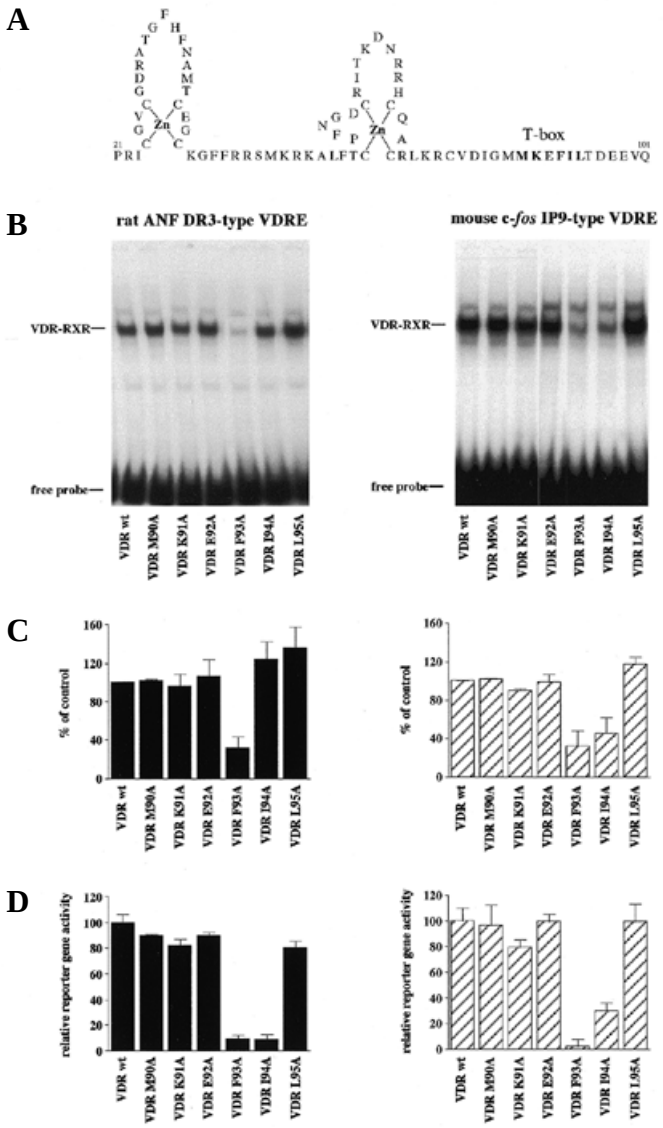

Figure 3. Importance of the VDR T-box for complex formation on DR3- and to IP9-type VDREs. The position of the T-box (indicated in bold) is schematically depicted in relation to the DBD of the VDR (**A**). Gel shift experiments were performed using *in vitro* translated VDR_{wt} or the indicated VDR T-box mutants VDR_{M90A}, VDR_{K91A}, VDR_{E92A}, VDR_{F93A}, VDR_{I94A} and VDR_{L95A} in combination with *in vitro* translated RXR on the ^{32}P-labelled rat ANF DR3-type VDRE or the mouse c-*fos* IP9-type VDRE. The experiments were performed at a salt concentration of 20 mM. VDR–RXR heterodimers were separated from free probe on a 5% non-denaturing polyacrylamide gel; a representative gel is shown (**B**). The relative amount of protein-complexed VDREs was quantified on a Bioimager. Columns represent means from triplicates and bars indicate standard deviations (**C**). Cos-7 cells were transfected with luciferase reporter constructs containing the DR3- or IP9-type VDRE, respectively, and expression vectors for VDR_{wt} (or the indicated VDR T-box mutants) and RXR. The cells were treated for 16 h with 100 nM VD or solvent (0.1% ethanol), then β-galactosidase-normalized luciferase activities were determined in relation to VDR_{wt} activity. Columns represent means from triplicates and bars indicate standard deviations (**D**).

The ligand-dependence of the heterdimerization of VDR_{wt} with RXR was then compared with that of VDR_{F93A}, VDR_{I94A} and their flanking mutations VDR_{E92A} and VDR_{L95A} on both VDRE types. The quantification of protein–DNA complex formation in relation to non-liganded VDR_{wt} is shown in Figure 4. Ligand-modulated protein–DNA interaction was found to depend on the ionic strength of the binding reaction and showed an optimal inducibility at a concentration of ~100 mM monovalent ions (K^+). Interestingly, on the DR3-type VDRE the formation of VDR_{wt}–RXR heterodimers was enhanced by 100 nM VD ~2-fold, whereas on the IP9-type VDRE the ligand stimulation was ~7-fold. Moreover, at this ionic strength the formation of non-liganded VDR_{I94A}–RXR heterodimers was found to be clearly reduced on both VDRE types, but the heterodimer

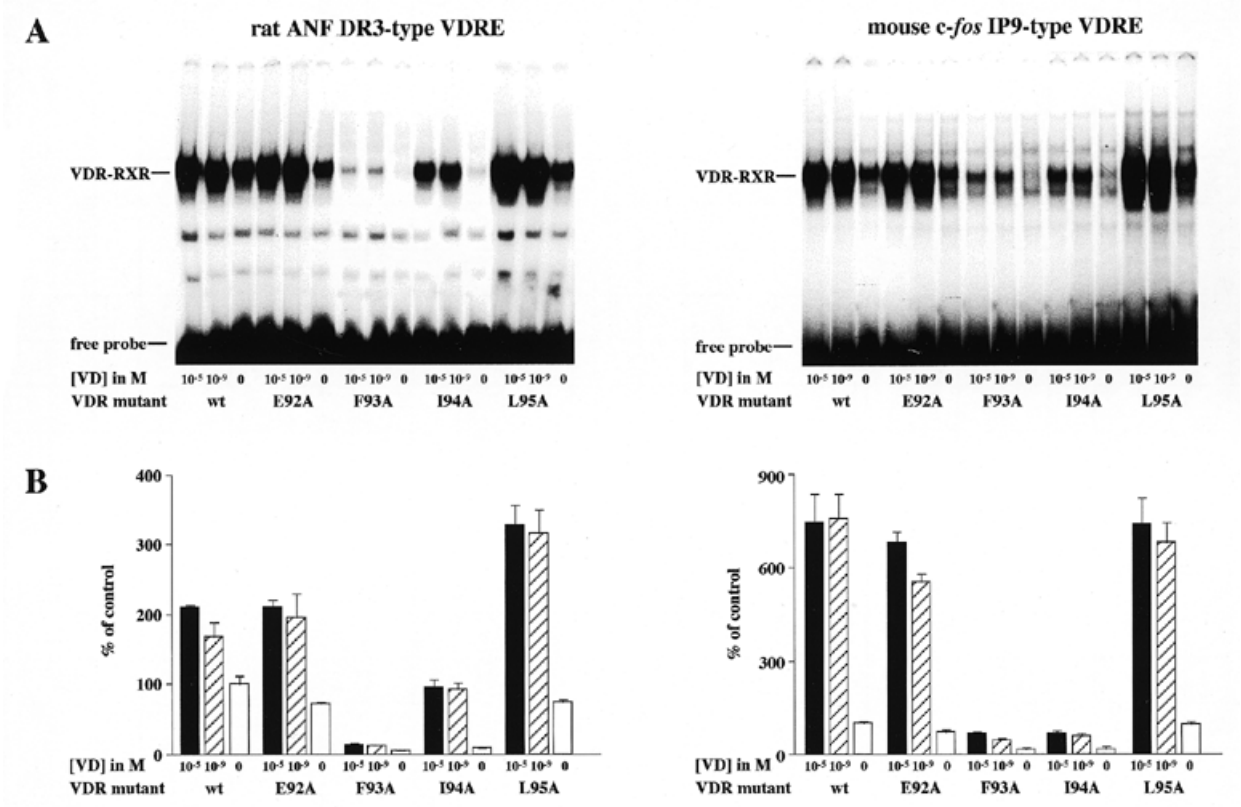

Figure 4. Ligand inducibility of VDR–RXR heterodimers *in vitro*. Heterodimers formed by *in vitro* translated VDR_{wt} (or the indicated VDR T-box mutants VDR_{E92A}, VDR_{F93A}, VDR_{I94A} and VDR_{L95A}) and *in vitro* translated RXR were preincubated with 10 µM VD, 1 nM VD or ethanol (as indicated). Gel shift experiments were performed either on the rat ANF DR3-type VDRE or the mouse c-*fos* IP9-type VDRE at an ionic strength of 100 mM KCl. VDR–RXR heterodimers were separated from free probe on a 5% non-denaturing polyacrylamide gel; a representative gel is shown (**A**). The amount of protein-complexed VDREs was quantified on a Bioimager in relation to non-liganded VDR_{wt}–RXR heterodimers. Columns represent means from triplicates and bars indicate standard deviations (**B**).

formation appeared to be more ligand-dependent on the DR3-type VDRE than on the IP9-type VDRE. Moreover, on the DR3-type VDRE the formation of VDR_{L95A}–RXR heterodimers demonstrated a clear ligand inducibility that was higher than that of VDR_{wt}–RXR heterodimers. In contrast, VDR_{E92A}–RXR and VDR_{F93A}–RXR heterodimers displayed a ligand inducibility that paralleled that of VDR_{wt}–RXR heterodimers on both VDRE types. However, in confirmation of the results shown in Figure 3C, the relative complex formation of VDR_{E92A}–RXR heterodimers was comparable with that of VDR_{wt}–RXR heterodimers, whereas that of VDR_{F93A}–RXR heterodimers was found to be clearly reduced.

Finally, the formation of non-liganded VDR_{I94A}–RXR heterodimers was compared with that of VDR_{wt}–RXR heterodimers on both VDRE types at salt concentrations varying from 20 to 150 mM KCl (Fig. 5). At low ionic strength, the F94 residue mutation did not affect heterodimer binding on the DR3-type VDRE, whereas a drastic effect on the binding on the IP9-type VDRE was seen, thus confirming the data shown in Figure 3C. However, on both VDRE types the amount of heterodimer formation between VDR_{I94A} and RXR was reduced with increasing ionic strength to almost undetectable levels. Interestingly, complex formation between VDR_{wt}–RXR heterodimers on the DR3-type VDRE initially increased upon elevating the ionic strength to 40 mM, then remained at a plateau with concentrations up to 80 mM, followed by a steady decrease in complex formation at higher ionic strength. In contrast, the respective complex formation on the IP9-type VDRE remained at a plateau when the ionic strength was between 20 and 60 mM and then decreased at concentrations >60 mM. Taken together, the data demonstrate that the influence of the I94A mutation on protein–DNA complex formation depends on both the ionic strength of the binding reaction and on the nature of the response element.

DISCUSSION

The different types of VDREs appear to be one of the important parameters for the different actions of the nuclear hormone VD. According to the model of multiple VD signalling pathways on each VDRE type, the VDR may assume a specific conformation and an individual interaction with ligand. In support of this model, some VD analogues (e.g. EB1089) have shown a tendency to preferentially activate VDR–RXR heterodimers that are bound to IP9-type VDREs (8), whereas other analogues (e.g. CB1093) seem to prefer DR3-type VDRE-bound VDR complexes (28). This indication of promoter selectivity may be correlated with the observation that IP9-type VDREs have been found in some genes that are involved in cell cycle regulation (21). In this way, the investigation of characteristic differences between DR3- and IP9-type VDREs is of central importance in understanding the molecular mechanisms of the pleiotropic hormone VD and for supporting the development of therapeutically potent VD analogues for targeting different genes.

Dimerization facilitates cooperative, high affinity interaction of nuclear receptors, such as VDR and RXR, with specific DNA

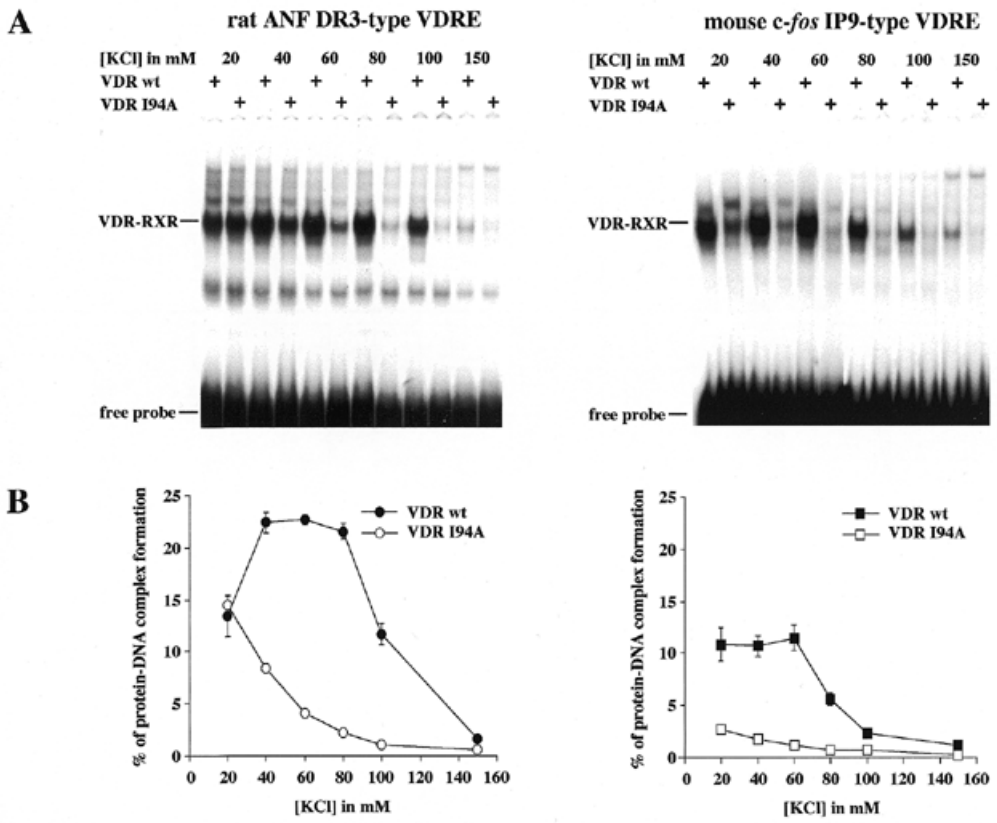

Figure 5. Ionic strength modulates the influence of the VDR T-box mutant VDR_{I94A} on VDR–RXR heterodimer complex formation. Gel shift experiments were performed using *in vitro* translated VDR_{wt} or the VDR T-box mutant VDR_{I94A} in combination with *in vitro* translated RXR on the ^{32}P-labelled rat ANF DR3-type VDRE or the c-*fos* IP9-type VDRE at the indicated ionic strengths. VDR–RXR heterodimers were separated from free probe on a 5% non-denaturing polyacrylamide gel; a representative gel is shown (**A**). The amounts of protein-complexed VDREs were quantified on a Bioimager. Each data point represents the mean of triplicates and bars indicate standard deviations (**B**).

recognition sites (29). As schematically depicted in Figure 2A, response elements that are formed by direct repeats force an asymmetrical binding of the heterodimeric partner receptors, whereas those that are formed by inverted palindromes allow a symmetrical arrangement of the receptors. However, on DR3-type VDREs, both receptor DBDs are located on roughly the same side of the DNA (tilted by 51.4°), whereas on IP9-type VDREs the DBDs are on nearly opposite sites of the DNA (tilted by 154.3°). Moreover, the distance between the DBDs along the axis of the DNA is three times higher on IP9-type VDREs than on DR3-type VDREs. It therefore seems remarkable that both VDRE types are specifically recognized by the same heterodimeric complex. However, the K_d value for the binding of VDR–RXR heterodimers to both VDRE types has been determined to be in a similar range of 0.5–1 nM (21,22). The efficient digestion of complexes on IP9-type VDREs compared with digestion on DR3-type VDREs in the gel shift clipping assay demonstrated that the extended DBDs of VDR and RXR do not contact each other on the IP9-type VDRE, whereas dimerization of the extended DBDs on the DR3-type VDRE stabilizes the protease-digested heterodimeric VDR–RXR complex on DNA. This observation was made both with *in vitro* translated VDR and bacterially expressed VDR and is the first experimental evidence that demonstrates that VDR–RXR heterodimers appear to be in a different conformation when they are bound to DR3-type VDREs than when bound to IP9-type VDREs.

The crystal structure of T_3R–RXR DBD heterodimers binding to a DR4-type response element (15) shows that residues of the T-box of the T_3R form salt bridges with residues of the DBD of RXR. Modelling of the DBDs of VDR and RXR that bind to a DR3-type VDRE was extrapolated on the basis of the T_3R–RXR structure (15). This modelling suggested that in the case of the VDR T-box, residues K91 and E92 form these salt bridges. However, neither K91 nor E92 is important for complex formation on both VDRE types, as shown in this study by *in vitro* binding assays and functional studies in transiently transfected cells. As the charged residues lysine and glutamine were replaced by a non-polar alanine residue, it seems unlikely that both were silent mutations, but, interestingly, highlights the limitation of stereochemical modelling. In contrast, the critical role of residue F93 in VDR–RXR heterodimer complex formation and VDR functionality on both DR3- and IP9-type VDREs described in this report confirms a previously published experimental study on the selectivity of the VDR for DR-type response elements (18). That study demonstrated that F93 is important for VDR homodimers to bind preferentially to DR3-type response elements in comparison to DR4- and DR5-type response elements. Moreover, it is interesting to note that in comparison with the other members of the nuclear receptor superfamily F93 is unique for VDR. Both the modelling (15) and the experimental study (18) provide data that are in agreement with the concept that the T-box contributes to the dimerization interface of the extended VDR DBD with the RXR

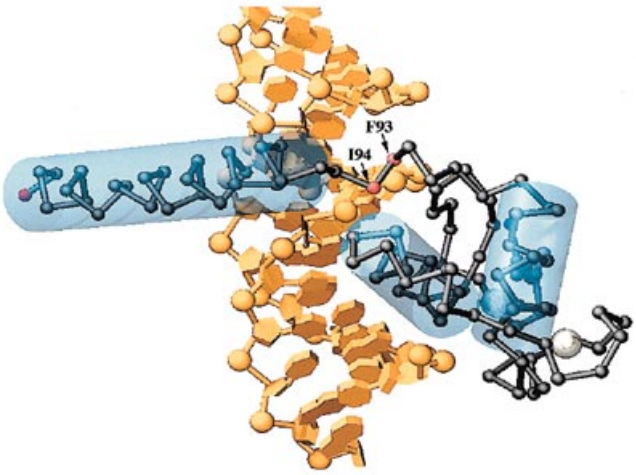

Figure 6. Location of the VDR residues F93 and I94. The amino acid sequences of the DBDs of human VDR and human $T_3R\beta$ show high homology. Therefore, the crystal structure of $T_3R\beta$ DBD (15) was used as a stereochemical model to visualize the position of the T_3R T-box residues that are homologous to the VDR residues F93 and I94 (red). They are located in a loop between the core DBD and the long α-helical structure of the hinge region. The α-carbon atoms of the polypeptide chain are shown, regions that form an α-helix are depicted by a light blue cylinder and the DNA is shown in yellow. Computer graphics were performed by translating the coordinates into constructive solid geometry (CSG) objects and subsequent ray tracing using the software POV Ray.

DBD, i.e. that on a DR3-type VDRE the VDR DBD appears to contact the RXR DBD directly. As indicated above, a direct contact of both DBDs is not possible on an IP9-type VDRE. The observation that F93 is also critical for complex formation between VDR–RXR heterodimers on IP9-type VDREs suggests that this residue has a function additional to its role as part of the dimerization interface. Interestingly, residue I94 was also shown in this study to have an important role in VDR–RXR heterodimer formation on both VDRE types. On a DR3-type VDRE, this residue could also be part of the dimerization interface, but on an IP9-type VDRE the same argument as for F93 holds true, i.e. I94 appears to have an additional function.

In order to get a visual impression of the locations of the F93 and I94 residues, a stereochemical model of the polypeptide backbone of the T_3R DBD (Fig. 6) was created on the basis of the coordinates of the T_3R–RXR DBD heterodimer crystal structure. As the DBDs of all members of the nuclear receptor superfamily are highly conserved, it can be assumed that the DBD of VDR appears structurally similar to that of T_3R. The model shows that both T-box residues are in a critical position for directing the orientation of the long α-helical part of the hinge region. This α-helix is rather rigid and appears to position the LBD on the other side of the DNA. A mutation of both F93 and I94 is therefore likely to change the orientation of the α-helix and in turn that of the LBD. This may influence the strong dimerization between the LBDs of VDR and RXR (30) and thus the whole DNA-bound VDR–RXR complex. In this respect, the observation that VDR–RXR heterodimers have a different stability on DR3- and IP9-type VDREs in response to the ionic strength of the solvent is very interesting, as this provides another, albeit indirect, argument that supports the concept that the overall structure of the two protein–DNA complexes is different (31). Taken together, F93 and I94 are not only the most critical residues of the T-box, but may also be critical in the context of the whole hinge region, as they not only have a role in the dimerization interface of the DBDs, but also appear to direct the relative orientation of the DBD to the LBD.

ACKNOWLEDGEMENTS

We would like to thank P. Polly for critical reading of the manuscript and for providing VDR_{GST} protein. This work was supported by the Medical Faculty of the Heinrich-Heine University Düsseldorf, the Fonds der Chemischen Industrie and the LEO Research Foundation.

REFERENCES

1 Carlberg,C. and Polly,P. (1998) *Crit. Rev. Eukaryotic Gene Expression*, **8**, 19–42.
2 Mangelsdorf,D.J., Thummel,C., Beato,M., Herrlich,P., Schütz,G., Umesono,K., Blumberg,B., Kastner,P., Mark,M., Chambon,P. and Evans,R.M. (1995) *Cell*, **83**, 835–839.
3 Carlberg,C. (1995) *Eur. J. Biochem.*, **231**, 517–527.
4 DeLuca,H.F., Krisinger,J. and Darwish,H. (1990) *Kidney Int.*, **38**, S2–S8.
5 Walters,M.R. (1992) *Endocr. Rev.*, **13**, 719–764.
6 Pols,H.A.P., Birkenhäger,J.C. and van Leeuven,J.P.T.M. (1994) *Clin. Endocrinol.*, **40**, 285–291.
7 Carlberg,C. (1996) *J. Invest. Dermatol. Symp. Proc.*, **1**, 10–14.
8 Nayeri,S., Danielsson,C., Kahlen,J.-P., Schräder,M., Mathiasen,I.S., Binderup,L. and Carlberg,C. (1995) *Oncogene*, **11**, 1853–1858.
9 Levin,A.A., Sturzenbecker,L.J., Kazmer,S., Bosakowski,T., Huselton,C., Allenby,G., Speck,J., Kratzeisen,C., Rosenberger,M., Lovey,A. and Grippo,J.F. (1992) *Nature*, **355**, 359–361.
10 Heyman,R.A., Mangelsdorf,D.J., Dyck,J.A., Stein,R.B., Eichele,G., Evans,R.M. and Thaller,C. (1992) *Cell*, **68**, 397–406.
11 Carlberg,C. (1996) *Endocrine*, **4**, 91–105.
12 Schräder,M., Nayeri,S., Kahlen,J.-P., Müller,K.M. and Carlberg,C. (1995) *Mol. Cell. Biol.*, **15**, 1154–1161.
13 Quélo,I., Kahlen,J.-P., Rascle,A., Jurdic,P. and Carlberg,C. (1994) *DNA Cell Biol.*, **13**, 1181–1187.
14 Schräder,M., Müller,K.M., Nayeri,S., Kahlen,J.-P. and Carlberg,C. (1994) *Nature*, **370**, 382–386.
15 Rastinejad,F., Perlmann,T., Evans,R.M. and Sigler,P.B. (1995) *Nature*, **375**, 203–211.
16 Lee,M.S., Kliewer,S.A., Provencal,J., Wright,P.E. and Evans,R.M. (1993) *Science*, **260**, 1117–1121.
17 Wilson,T.E., Paulsen,R.E., Padgett,K.A. and Milbrandt,J. (1992) *Science*, **256**, 107–110.
18 Towers,T.L., Luisi,B.F., Asianov,A. and Freedman,L.P. (1993) *Proc. Natl Acad. Sci. USA*, **90**, 6310–6314.
19 Zechel,C., Shen,X.-Q., Chen,J.-Y., Chen,Z.-P., Chambon,P. and Gronemeyer,H. (1994) *EMBO J.*, **13**, 1425–1433.
20 Carlberg,C., Bendik,I., Wyss,A., Meier,E., Sturzenbecker,L.J., Grippo,J.F. and Hunziker,W. (1993) *Nature*, **361**, 657–660.
21 Schräder,M., Kahlen,J.-P. and Carlberg,C. (1997) *Biochem. Biophys. Res. Commun.*, **230**, 646–651.
22 Kahlen,J.-P. and Carlberg,C. (1996) *Biochem. Biophys. Res. Commun.*, **218**, 882–886.
23 Allan,G.F., Leng,X., Tsai,S.Y., Weigel,N.L., Edwards,D.P., Tsai,M.-J. and O'Malley,B.W. (1992) *J. Biol. Chem.*, **267**, 19513–19520.
24 Leng,X., Tsai,S., O'Malley,B.W. and Tsai,M.-J. (1993) *J. Steroid Biochem. Mol. Biol.*, **46**, 643–661.
25 Peleg,S., Sastry,M., Collins,E.D., Bishop,J.E. and Norman,A.W. (1995) *J. Biol. Chem.*, **270**, 10551–10558.
26 Nayeri,S. and Carlberg,C. (1997) *Biochem. J.*, **235**, 561–568.
27 Nayeri,S., Kahlen,J.-P. and Carlberg,C. (1996) *Nucleic Acids Res.*, **24**, 4513–4519.
28 Danielsson,C., Mathiasen,I.S., James,S.Y., Nayeri,S., Bretting,C., Mørk Hansen,C., Colston,K.W. and Carlberg,C. (1997) *J. Cell. Biochem.*, **66**, 552–562.
29 Gronemeyer,H. and Moras,D. (1995) *Nature*, **375**, 190–191.
30 Nishikawa,J.-i., Kitaura,M., Imagawa,M. and Nishihara,T. (1995) *Nucleic Acids Res.*, **23**, 606–611.
31 Gewirth,D.T. and Sigler,P.B. (1995) *Nature Struct. Biol.*, **2**, 386–394.